Mechanical properties and Keratinocytes cellular evaluation of Polycaprolactone/Collagen/Elastin Electrospun Fiber Scaffolds

Y.E. Aguirre-Chagala, V. Altuzar, Hiram Isaac Beltrán, S. Muñoz-Aguirre, E. Garrido,
R. Ruiz-Ramos, C. Mendoza-Barrera

Bioinspired membranes as extracellular matrices are desired for skin regeneration. Herein, we fabricate four systems of fibrillar membranes composed of polycaprolactone (PCL), aminolyzed PCL, denatured collagen type I (C), and the blend of collagen hydrolysate types I and III (bC) or elastin (E), fabricated by the electrospinning process. The superficial features by SEM and optical profilometry, mechanical properties by puncture strength assays, and biological evaluation with a human keratinocyte cell line (HaCaT) for one day of aPCL6bCE (aPCL/collagen hydrolysate type I and III/Elastin), aPCL6CE (aPCL/denatured Col I/elastin), aPCL6bC (aPCL/collagen hydrolysate type I and III), and PCL6bCE (PCL/collagen hydrolysate type I and III/Elastin) membranes are described. The aPCL6bCE and aPCL6CE fibers resulted in better structural properties for culturing cells, while aPCL6bC and PCL6bCE membranes have shown lower viability for keratinocytes, probably due to their different chemical surface and nanotopography. The roughness of these materials varied from 4.53 to 114.4 µm, depending on their diameter values. Puncture strength results were not significantly different within 2.25–2.66 MPa. Our results suggest that aPCL6bCE and aPCL6CE fibers have potential applications in skin tissue engineering, where the synergy among aminolyzed PCL and E seems to be a prerequisite to developing such activity.

Introduction

Tissue engineering is an important area that requires an artificial extracellular matrix (ECM). Skin is the non-homogeneous, viscoelastic, anisotropic, and more extensive material in the body, constituting about 15% of the total mass and is composed of three layers: epidermis, dermis, and hypodermis, and a thickness range of 0.4–2.6 mm across different body locations. The epidermis (thickness of 0.5–1 mm) and dermis (thickness of 1–4 mm) have nerves and blood vessels [1]. The epidermis has a high cell structure composed of keratinocytes and melanocytes; meanwhile, the dermis consists of an ECM constituted by collagen (types I and III), elastin, reticulin, hyaluronan, and proteoglycans, where cells are primarily fibroblasts and endothelial cells [2].

There are diverse causes of skin damage, such as genetics, surgical interventions, or injuries, one of the most common is thermal lesions. Skin regeneration and healing is a complex natural process that requires the migration, proliferation, and differentiation of keratinocytes and fibroblasts. When the injury is too deep, the skin cannot regenerate itself. For its regeneration, grafted scaffolds are necessary to favor cellular growth. A problem with the clinical implant of the substituted dermis is its low adherence, insufficient vascularization, subsequent infection, and, therefore, the partial necrosis of the substituted dermis [3].

For this reason, the regeneration of the whole thickness of the skin has been a current challenge because tissue vascularization and the growth of hair follicles are hardly produced in the grafted scaffolds. Skin transplantation is of great interest for people wounded by burns [4]. A wound of 4 cm will not be self-sufficient to regenerate and scar; for those cases, healing could be possible by grafting.

Collagen and elastin are among the main components of the skin. Both biopolymers contribute to the biomechanical properties of this tissue, where collagen is responsible for the strength and elastin for the resilience [5]. Furthermore, collagen is the most abundant protein in the human body and is responsible for maintaining the total integrity of vertebrates [6]. Hence, this protein possesses superior properties to synthetic polymers, such as good biocompatibility, biodegradability, and low antigenicity [7-10]. Because of these significant features, collagen has been extensively used to fabricate artificial ECM [10,11]. Another robust polymer is polycaprolactone (PCL), a synthetic biocompatible polyester widely used in biomedical applications. PCL is hydrophobic, with a long biodegradation period, and is commonly employed with

Yanet E. Aguirre-Chagala 🔴
*Centro de Investigación en Micro y Nanotecnología,
Universidad Veracruzana
Boca del Río, Veracruz, 94294, México.*

Victor Altuzar 🔴, Severino Muñoz-Aguirre 🔴,
Claudia Mendoza-Barrera ✉🔴
*Facultad de Ciencias Físico-Matemáticas,
Benemérita Universidad Autónoma de Puebla
Puebla, Puebla, 72570, México.*

Hiram Isaac Beltrán 🔴
*Departamento de Ciencias Básicas, DCBI, Universidad Autónoma Metropolitana, Unidad Azcapotzalco
Azcapotzalco, Cd. de México, 02200, México.*

Efraín Garrido 🔴
*Departamento de Genética y Biología Molecular,
Centro de Investigación y de Estudios Avanzados, I.P.N.
Gustavo A. Madero, Cd. de México, 07360, México.*

Rubén Ruiz-Ramos 🔴
*Facultad de Medicina, Universidad Veracruzana
Veracruz, Veracruz, 91700, México.*

other biopolymers to tune the final physicochemical properties of the resulting composite material [12,13].

Moreover, fibers are composite materials widely applied in tissue engineering because their structure serves as artificial ECM [14,15]. In particular, the electrospinning process is a versatile method to produce fibers, not only controlling sizing at micro and nanoscales but also primarily utilized in tissue engineering due to the development of high porosity and surface enhancement, two critical factors to seed cells therein [16,17].

In previous work [13], we reported the fabrication and physicochemical and mechanical properties of denatured collagen type I, elastin, PCL, or aminolyzed PCL (a-PCL) fibers fabricated by electrospinning at several concentrations and combinations. Fibers were labeled as aPCLXCE and aPCLXbCE, where X is the ratio of fed aPCL (100:0:0, 90:5:5, 80:10:10, 64:18:18, or 50:25:25); C is the denatured collagen type I; bC is the blend of collagen hydrolysate type I and III; and E indicates elastin. PCL fibers were fabricated as control. It was found that PCL, aPCL (relation 100:0:0), and aPCL5CE (relation 50:25:25) samples exhibited one group of fibers, whereas aPCL9CE, aPCL8CE, and aPCL6CE showed two average diameters. PCL fibers exhibited a rough surface on the microscale, whereas aPCL ones presented flat and smooth ribbons with their thickness on the nanoscale. On its side, C and E in the fibers strongly influenced their morphology. aPCL9CE, aPCL8CE, and aPCL6CE showed the presence of thick and thin mixed fibers in different concentrations, whereas aPCL5CE had net-like morphology. Quantification of amino groups in all fabricated samples containing aPCL increased their NH_2/mg content. The highest content of 21 mM NH_2/mg fiber of amino groups corresponded to the relation 64:18:18 (aPCL6CE sample), followed by 70:15:15 (aPCL7CE), 50:25:25 (aPCL5CE), 80:10:10 (aPCL8CE), 90:5:5 (aPCL9CE), and 100:0:0 (aPCL) with 18.8, 16.9, 8.2, 5.9, and 0.36 mM NH_2/mg fiber, respectively. Also, they showed denaturation of collagen conformation throughout the change of amide I and unfolded structure of amide II; and the denaturation of the secondary structure of the E protein. Because of the highest NH_2/mg fiber content, was selected the aPCL6CE-based system to study their morphology, swelling, hydrophilicity, micromechanical, and thermal properties. Binary and ternary systems of the group under study included aPCL, aPCL6E, aPCL6bC, aPCL6CE, aPCL6bCE, and PCL6bCE systems. The morphology studies and the determination of average diameters of the systems showed that using E for fiber formation (aPCL6E) bestows more parallel staking-type fibers of ~322 nm. aPCL6bC fibers exhibited a fluffy and aleatory fiber arrangement with a rough fiber surface with an average diameter of 293 nm with a narrower distribution. Using a blend of collagen hydrolysate type I and III (aPCL6bCE system) promoted the formation of homogeneous morphology with protuberances on fiber surfaces with a mean diameter close to 484 nm instead of two groups. The difference between aPCL6CE and aPCL6bCE samples was the collagen's folded and unfolded structures, where the raw bC precursor presented the formation of tyrosine from

phenylalanine (aging of collagen). Finally, the PCL6bCE system showed striated tubular fibers with the highest average diameter ~693 nm. Then, the presence of aPCL promotes more intermolecular forces caused for the amide and amino bonds leading to small diameters. All systems showed about 320% swelling in 24 h, indicating an excellent capability to preserve the structure; nevertheless, the aminolyzed PCL-based system (aPCL) presented the highest water absorption (~600%). Then, we suggested that exposing -NH_2 terminals on aPCL fibers strongly enhances its ability to contain water. On its side, a modulated diffusivity of the aqueous phase can be achieved by the optimal selection of components of each fiber system. We found that the aPCL6CE system showed the most hydrophilic membrane (17°), followed by both aPCL6bCE and aPCL6bC (42.4°), aPCL (71.5°), PCL6bCE (80°), whereas the aPCL6E sample was the less hydrophilic (108.3°). The thermal analysis determined that the combined presence of aPCL, collagen type I, and E (aPCL6CE system) conferred the highest thermal resistance (170 °C) and more crystallinity, followed by the use of aPCL, collagen hydrolysate type I and III, and E (aPCL6bCE sample with 148 °C). The presence of additional bC or E biopolymers (aPCL6bC and aPCL6E samples) also increased their thermal properties at 133° and 115°, respectively. In all cases, T_m was kept around 59.7–61.3 °C. In the individual fibers micromechanical tests, discarding their properties in bulk, the elasticity modulus values were from 0.5, 0.8, 1.8, and 3.04 GPa for aPCL6CE (397 nm), aPCL6bCE, aPCL6C, and PCL6bCE samples, respectively. Then, the fabricated PCL-based fiber systems showed suitable physicochemical and mechanical properties for enhanced biological activity for several biomedical applications and tissue scaffold engineering.

Due to all the latter statements, this work aimed to investigate the biofunctionality of aPCL6CE (aPCL/denatured Col I/Elastin), aPCL6bCE (aPCL/denatured Col I/Col I+Col III/Elastin), aPCL6bC (aPCL/Col I+Col III) and PCL6bCE (PCL/ Col I+Col III/Elastin) biopolymeric fibrous membranes for their use in tissue engineering by determining their mechanical properties, superficial features, and biological evaluation in HaCaT cell cultures.

Materials and Methods

Materials

Polycaprolactone (PCL; M_w = 80,000), 1-4 dioxane (DIOX), hexamenthylendiamine (HMDA), collagen type I from bovine Achilles tendon (C), 1,1,1,3,3,3-hexafluoro-2-propanol (HFIP) were purchased from Sigma. Isopropanol (ISOP) and elastin (E) were obtained from MP Biomedicals, LLC; collagen hydrolysate types I and III (bC) were purchased from Neocell. These materials were used to fabricate the fiber by electrospinning process, as previously described [13]. Dulbecco's modified eagle medium (DMEM) was purchased from Sigma Aldrich Chemical, Co. (St. Louis, MO, USA); deionized water and ethanol were obtained from HYCEL of Mexico S.A. de C.V.; Trypsin, Penicillin-streptomycin, Sodium pyruvate, Fetal bovine

serum, and L-glutamine, were purchased from Invitrogen-Thermo Fisher Scientific (Carlsbad, CA, USA). All chemical reagents were used as received unless otherwise specified.

Sample preparation

aPCL6CE (aPCL/denatured Col I/Elastin), aPCL6bCE (aPCL/denatured Col I/Col I+Col III/Elastin), aPCL6bC (aPCL/Col I+Col III) and PCL6bCE samples were fabricated similarly to our previous work [13]. Briefly, PCL was aminolyzed, collagen type I was denatured, collagens type I and III blended by hydrolysis, whereas E was used as was purchased. The electrospun solutions are 0.064 g of aPCL or PCL dissolved in 1mL of HFPI in a sealed beaker under magnetic stirring. Then, 0.018 g of C or bC and 0.018 g of E are added and dissolved overnight to obtain precursor solutions. In the case of aPCL6bC solution, is used 0.36 g of bC. The polymer solution of interest was injected at 0.25 mL/h (KD scientific™, model: 780100V). The applied voltage V = 20 kV was supplied (Gamma High Voltage Research, model: ES60p-20W/DAM) between a stainless steel needle (21Gx32 mm) used as the anode, and the cathode of the circuit was connected to a rotary collector (at 21,000 rpm) with six tips forming a semicircle of 9 cm in diameter and 5 cm in height. The needle - collector separation was d = 7 cm, in a chamber with RH = 35%–50% of relative humidity. The fabricated fibers were vacuum-dried for 24 h to remove the traces of solvent and stored in a desiccator. All samples were replicated 5 times.

Characterization

Images of the electrospun composites were obtained with a JEOL model JSM-7600F scanning electron microscope. Fiber samples were prepared by placing a conductive carbon double-sided tape. The voltage and magnification used to analyze all samples were 0.5 kV and 3,000X, respectively.

The film thickness (µm) was determined for four films averaging measurements at five points for each film using a hand-held microcalliper (Mitutoyo Corp, Kawasaki, Kanagawa, Japan). Thickness measurements were taken to calculate the values of puncture strength.

The topographic roughness parameters (Ra) of membranes were measured through noncontact optical profilometry using an interferometer profiler (Wyko–Veeco, model NT9100, USA) in Vertical Scanning Interferometry Mode, equipped with the WycoVision® 32 analytical software. The roughness parameters were measured in nine different regions (Magnification 5X and 20X) for each sample.

Fibrous membranes with a diameter of 2 cm were fixed in a self-designed acrylic holder plate with a 1 cm hole. The puncture strength of the films was measured with a puncture test using a Texture analyzer (TA.XT. Plus texture analyzer, Stable Micro Systems Ltd., UK, and Exponent 5.1.1.0 software). A metal probe P5S with a hemispherical end (diameter 3 mm) was driven through the dry film at a speed of 1 mm/s. Force (N) versus displacement (mm) curves were recorded with a 5 g load cell. The Puncture strength (PS) was calculated as:

$$PS = \frac{F_{max}}{A_{CS}}$$

where F_{max} is the maximum applied force at membrane break, A_{CS} is the cross-sectional area of the edge of the membrane located in the path of the cylindrical hole of the membrane holder plate ($A_{CS} = 2r\delta$), and where r is the radius of the hole and δ is the thickness of the membrane).

Cellular viability and proliferation analysis on the fibrous membranes was evaluated in a biosafety cabinet Purifier Logic Class II using HaCaT cells, which are immortalized human keratinocytes and have been extensively used to study epidermal homeostasis and its pathophysiology [18]. The fibers were sterilized under UV light for 15 min; their immersion was in a 24-well cell culture disposable flask (Corning, NY, USA). A coverslip was used to adhere the fibers with an epoxy resin, frequently used in confocal microscopy, to ensure a complete immersion into the culture media. Then, 4.0×10^5 cells were seeded per well along 12 wells, each type of fiber was assayed by triplicate, using two controls, and the setup time for this experiment was 24 h. All cells were grown at 37 °C in a humidified atmosphere of 5% CO_2. Once cellular proliferation reached a confluence point, the fibers were removed from the wells, and cells were fixed by immersion of fibers into 2 mL of formaldehyde solution (10%) for 10 min. Subsequently, cells were stained with Harris's hematoxylin for 5 min. Later, they were dehydrated through immersion on a progression of ethanol (from 30% to 100%) for 2 min each, then cleared with xylenes for 2 min, and finally mounted with the synthetic epoxy resin (EPON, Hexion) on a slide. Analysis of cellular attachment was done by optical microscopy.

Data were analyzed by one-way analysis of variance (ANOVA) in conjunction with Tukey's post hoc test for multiple comparisons. Differences were considered with significance at $p < 0.05$.

Results and discussion

In the present work, four fiber membranes composed of polycaprolactone (PCL), aminolyzed PCL (aPCL), denatured collagen type I (C), the blend of collagen hydrolysate types I and III (bC) or elastin (E) were fabricated by the electrospinning process by an analog procedure previously reported [13]. The HaCaT cell line was cultured in vitro into the fabricated systems to verify the scaffold viability. A central feature of tissue scaffolds is the structure in which cells interact with the material. These microstructural features will be discussed forthcoming.

SEM micrographs and optical profilometry confirmed that the fabricated membranes developed characteristic tridimensional arrangements showing randomly distributed fibrillar structures (Figure 1), particularly aPCL6bCE (Figure 1a), which presented a flattened ribbon type structure, sometimes ranging from 1 or 2 strands per ribbon with large randomly distributed interspaces. Comparatively, PCL6bCE (Figure 1b) developed a thicker ribbon structure ranging 2 or 3 strands per ribbon, more commonly three strands. And for the latter two cases, aPCL6bC (Figures 1c, 1g, 1k) and aPCL6CE (Figure 1d), both were of single-strand nature, and particularly the last is the one with the most
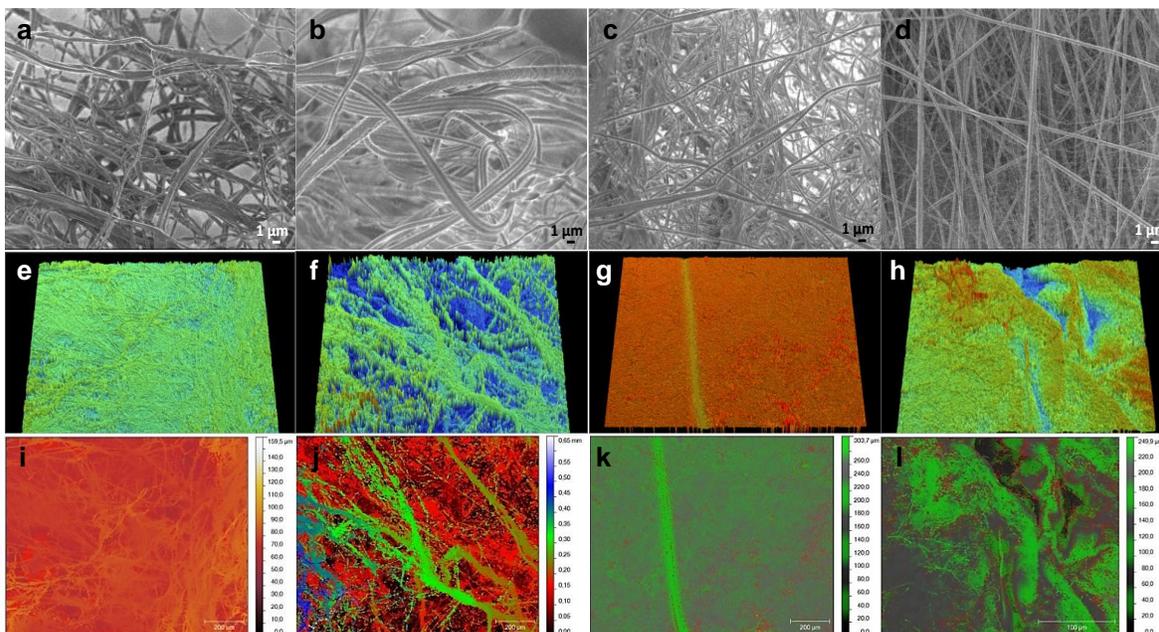
Figure 1. SEM images: (a) aPCL6bCE, (b) PCL6bCE, (c) aPCL6bC and (d) aPCL6CE. Scale bars in the inset micrograph correspond to 1 μm, and 0.5 kV. Below each micrograph is presented their corresponding optical profilometry images at 5X: (e-h) tridimensional and (i-l) topography images. The color scale corresponds to μm (i and k) and mm (j), respectively.

homogenous transversal section. In all cases, the lengths of fibers are above 100 μm, according to 100×100 μm² micrograph scaling. All yarn samples differed mainly in their average diameter values ranging from 293 nm to 693 nm. In particular, the average diameters were from 484 ± 107 nm for aPCL6bCE, 693 ± 273 nm for PCL6bCE, 293 ± 105 nm for aPCL6bC. Specifically, for the aPCL6CE sample, two distributions were obtained between 397 ± 100 nm and 84 ± 20 nm. The morphology of these specimens was more ruffled for aPCL6bCE, PCL6bCE, and aPCL6bC, see Figure 1(a-c), all containing collagen hydrolysate type I and III. For the case of aPCL6CE, a more straight and aligned morphology was observed. In Figure 1b, it could be observed that the diameter of the composite is enhanced; this occurs when non-aminolyzed PCL is employed. In Figure 1c, sample without elastin, and Figure 1d, sample with elastin, the latter resulted thicker but with two size distributions. While comparing Figure 1(a-c), collagen hydrolysate type I and III, and Figure 1d, with denaturated Col I, the former three developed ribbed fibers, and the latter single flattened surfaces. These results are in concordance with those previously reported in [13].

Optical profilometry was used to determine the roughness of the samples (Figure 1 (e-l)). The thickness of the prepared films ranged from 102 to 277 μm. The topography is essential for determining how the cells interact with these scaffolds. In the case of aPCL6CE, the roughness was 11.98 ± 0.65 μm, which might be attributed to the thick and thin fibers forming this scaffold. As was expected, the PCL6bCE thread had the highest roughness of 114.4 ± 5.0 μm, correlating this value with the greatest fiber diameter of 693 nm and, therefore, the largest porous sizes [13]. Lower roughness was obtained for aPCL6bCE and aPCL6bC, which presented 4.53 μm and 3.35 μm,

respectively. Then, the roughness decreased with the decrease of the diameter of the initial fiber, except for the aPCL6bCE sample. However, it relays in the same order of magnitude as their aPCL-containing analogs.

Mechanical Properties

The mechanical properties of the four fiber samples were tested by puncture strength (PS) measurements in the quasistatic regime (Table 1).

aPCL6bCE fiber has shown a PS of about 2.54 MPa, practically the same PS compared with PCL6bCE fiber (2.25 ± 1.41 MPa). Even though segments of aPCL were shorter than the unmodified PCL chains in the blend, it did not cause a significant difference in mechanical strengths. For aPCL6bCE and aPCL6CE fibers, there was no significant effect over PS (2.54 MPa versus 2.66 MPa, respectively), in which the 64 wt% of aPCL in both could explain this trend. Moreover, when elastin is not loaded in the fiber system (aPCL6bC), PS was 2.78 MPa. Then, the fiber system is a little more resistant. Nevertheless, regardless of their components, the four fibrous membranes fabricated did not exhibit a remarkable variance in their PS values.
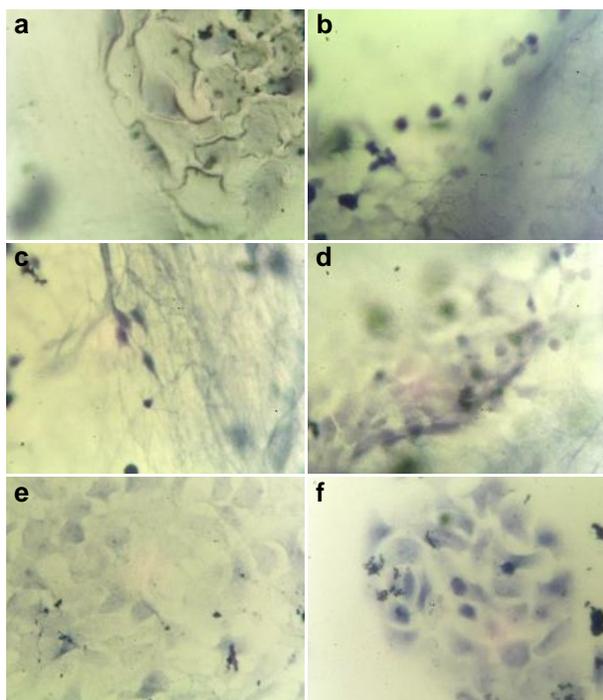
It has been reported that the dermis is composed of papillary and reticular layers, contributing, more than the

Table 1. Physical properties of the electrospun membranes.

Fiber	Thickness (μm)	Puncture strength (MPa)	Roughness (μm)
aPCL6bCE	135 ± 18	2.54 ± 0.82	4.53 ± 0.50
PCL6bCE	277 ± 67	2.25 ± 1.41	114.4 ± 5.0
aPCL6bC	161 ± 21	2.78 ± 1.84	3.35 ± 0.55
aPCL6CE	102 ± 16	2.66 ± 1.21	11.98 ± 0.65

epidermis, to the mechanical properties of the skin. The randomly oriented collagen type I fibers of the papillary layer (0.3–3.0 mm) contain packed thinner ones (20–40 nm); meanwhile, the interwoven, wavy, randomly oriented collagen type I and III bundles of the reticular layer range from 10 µm to 40 µm in diameter [19]. SEM showed that the fabricated samples have the average diameter, porosity, and morphology of the papillary dermis layer instead of the reticular stratum. Besides, profilometry (Figure 1) confirmed their high porosity, with their roughness close to the depth of sulci cutis reported for human skin [20]. Also, it has been reported that Young's skin modulus depends on the area, posture, gender, and age [21]. This behavior is explained because collagen is the load-carrying element with intramolecular crosslinks giving strength to the skin, whereas elastin provides its elasticity. With age, the density and orientation of these fibers change, leading to a considerable decrease in elasticity. Khaothong [22] and Zheng and Mak [23] found, for quasistatic experiments (0.5–1 mm/s), values of PS of 0.1–2.4 MPa, and 10.4–89.4 kPa for inner-forearm and tibia/fibula skins. Because aPCL6CE, aPCL6bCE, aPCL6bC, and PCL6CE samples showed a swelling behavior between 305% to 400%, hydrophilic surfaces with contact angles between 17° and 80°, at least 21 mM NH_2/mg fiber of amino groups exposed, a T_m between 59.7 °C and 61.3 °C [13], and suitable morphological and mechanical properties of skin, they can serve as potential skin cell reservoirs.

The biocompatibility of the four systems was evaluated in vitro by human keratinocytes for 24 h of cell culture (Figure 2) spread over the fibers. The presence of stained cells within fibrous scaffolds was observed by optical microscopy. It was
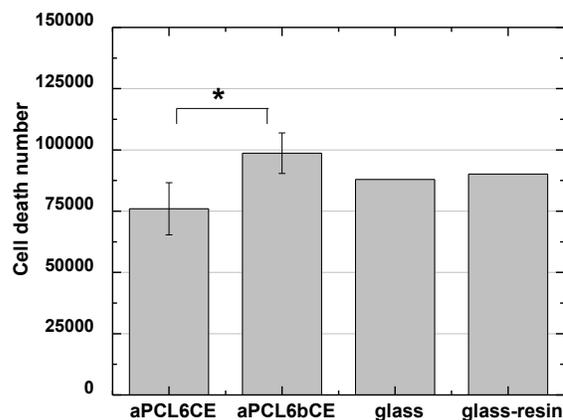
noticed that keratinocytes were spread over aPCL6bCE fiber, keeping populations of HaCaT cells with cobblestone formation in some regions of this 3D nanofibrillar membrane, Figure 2a [24]. Keratinocytes morphology was affected according to the nanotopography of this fibrous support; see Figure 1a [25]. By detecting their nuclei, it was observed that they adopt a flattened extended shape connected to each other. Besides the guidance of the nanotopography on cell morphology, the contribution of 34 wt% of collagen-elastin and aPCL could have had an important role. Therefore, the cell viability was as good as expected (see Figure 3), with 24% dead cells after one day, which is a very acceptable value derived from the natural cellular process.

Interestingly, the cells cultured on PCL6bCE fiber (Figure 2b) were not successfully attached; as a result, dead cells were identified according to their rounded morphology and tiny sizes. Contrarily, glass (Figure 2e) as control reached 22% of dead cells. Likely, this opposite upshot could be ascribed to the larger interfibrillar pores of PCL6bCE fiber, which are unsuitable surfaces for living guests within 3D scaffolds. Even though collagen and elastin were used as precursors, they are not enough requisites to favor cell attaching [26,27]. In addition, as reported, those greater diameters stimulate smaller cell sizes derived from the lack of interlinking [28].

Similar to PCL6bCE, on aPCL6bC fiber (Figure 2c), cells were entrapped throughout the fibrillar material with an inadequate topography to attach them, proving its low viability to interact with keratinocytes [29]. As stated, this type of cell behavior on the scaffolds (aPCL6bC and PCL6bCE) resulted from insufficient intercellular contact.

On the other hand, the aPCL6CE fiber had good biocompatibility and cell viability of 19% (Figures 2d & 3), possibly because it had two different types of fibers, which would improve the interaction with cells. The presence of both yarns allowed the tiny fibers to connect to the larger ones, generating a better tangle/mesh and thus favoring a better connection with cellular surfaces and biomaterials, which enhanced the density of cells on the matrix. It should be noted that there was a better distribution of keratinocytes all over the material, as illustrated (Figure 2d), but this was

Figure 2. Optical microscopy images at 40X of human keratinocytes stained after 24 h. (a) aPCL6bCE, (b) PCL6bCE, (c) aPCL6bC, (d) aPCL6CE, (e) glass and (f) glass with epoxy resin; these last two were used as controls.

Figure 3. Cell death count comparison between fibers and control ($*p < 0.05$).

because the multilayer formation of the images under optical microscopy was unfocused on some points.

As has been herein observed, arrangements of fibers and contact surfaces are essential issues in tissue engineering. In general, we are able to say that due to the randomly fluffy structure of these materials, it is difficult to spread it all over the HaCaT cells. More cellular spreading has been observed when HaCaT cells are supported onto flat surfaces, growing more readily because there is more surface area and, thus, contact with the support. A tridimensional environment is adequate for tissue engineering to infiltrate, grow, and spread cells. However, as it was seen for HaCaT, cells should be attached more straightforwardly on dense surfaces but with a well-tuned tangle/mesh. In addition to what was mentioned before, another factor that might influence is the number of available amino groups interacting with cells, modifying the bioactivity [30,31]. Both aPCL6bC and PCL6bCE demonstrated low viability compared to aPCL6bCE and aPCL6CE samples. This latter could be attributed to their wettability since aPCL6bC, and PCL6bCE showed 71.5° and 80°, respectively, whereas aPCL6bCE and aPCL6CE presented 42.4° and 17°, respectively being the latter more suitable due to their high wettability correlating with cell viability [8,13]. Therefore, more cell growth viable systems should be obtained with the combination of aPCL and E, and the variation of the collagen type could modulate variable degrees of wettability.

Conclusions

Structural, wettability, nanotopography, and mechanical and chemical properties strongly influenced cellular activity. The materials with optimal properties for culturing human keratinocytes were aPCL6CE and aPCL6bCE samples. It can be said that the fibers fabricated with aminolyzed PCL plus elastin, with some collagen, as components were promising scaffolds. This latter was mainly due to the combination of two threads, thinner and thicker, generating a well-tuned tangle/mesh with high wettability. Therefore composite materials fulfilling these features could be important candidates for skin replacement trials.

Acknowledgments

References

[1]. F. Groeber, M. Holeiter, M. Hampel, S. Hinderera, K. Schenke-Laylandac, *Adv. Drug Deliv. Rev.* **63**, 352 (2011).
[2]. J.K. Kular, S. Basu, R.I. Sharma, *J. Tissue Eng.* **5**, 1 (2014).
[3]. S. MacNeil, *Nature* **445**, 874 (2007).
[4]. A.D. Metcalfe, M.W.J. Ferguson, *J. R. Soc. Interface* **4**, 413 (2007).
[5]. Q. Chen, S. Liang, G.A. Thouas, *Prog. Polym. Sci.* **38**, 584 (2013).
[6]. R. Parenteau-Bareil, R. Gauvin, F. Berthod, *Materials* **3**, 1863 (2010).
[7]. C. Chaubaroux, E. Vrana, C. Debry, P. Schaaf, B. Senger, J.C. Voegel, Y. Haikel, C. Ringwald, J. Hemmerlé, P. Lavalle, F. Boulmedais, *Biomacromolecules* **13**, 2128 (2012).
[8]. D. Grafahrend, K.H. Heffels, M. Möller, D. Klee, J. Groll, *Macromol. Biosci.* **10**, 1022 (2010).
[9]. J.L. García, A. Asadinezhad, J. Pacherník, M. Lehocký, I. Junkar, P. Humpolíček, P. Sáha, P. Valášek, *Molecules* **15**, 2845 (2010).
[10]. B.S. Kim, I.K. Park, T. Hoshiba, H.L. Jiang, Y.J. Choi, T. Akaike, C.S. Cho, *Prog. Polym. Sci.* **36**, 238 (2011).
[11]. S.A. Sell, P.S. Wolfe, K. Garg, J.M. McCool, I.A. Rodriguez, G.L. Bowlin, *Polymers* **2**, 522 (2010).
[12]. M.A. Woodruff, D.W. Hutmacher, *Prog. Polym. Sci.* **35**, 1217 (2010).
[13]. Y.E. Aguirre-Chagala, V. Altuzar, E. León-Sarabia, J.C. Tinoco-Magaña, J.M. Yañez-Limón, C. Mendoza-Barrera, *Mater. Sci. Eng. C* **76**, 897 (2017).
[14]. A.L. Butcher, G.S. Offeddu, M.L. Oyen, *Trends Biotechnol.* **32**, 564 (2014).
[15]. B. Dhandayuthapani, Y. Yoshida, T. Maekawa, D.S. Kumar, *Int. J. Polym. Sci.* **2011**, 1 (2011).
[16]. Q.L. Loh, C. Choong, *Tissue Eng. Part B Rev.* **19**, 485 (2013).
[17]. J.R. Venugopal, R. Sridhar, R. Rajeswari, M. Shayanti, B. Ramalingam, S. Subramanian, R. Seeram, *Wound Repair Regen.* **21**, 1 (2013).
[18]. M.R. Matus-Muñoz, R. Ruiz-Ramos, V. Altuzar, H.I. Beltrán, M.A. Palomino-Ovando, C. Mendoza-Barrera, *Int. J. Polym. Mater. Polym. Biomater.* **2021**, 1 (2021).
[19]. F.H. Silver, J.W. Freeman, D. DeVore, *Skin Res. Technol.* **7**, 18 (2001).
[20]. R. Ohtsuki, T. Sakamaki, S. Tominaga, *Opt. Rev.* **20**, 94 (2013).
[21]. A. Kalra, A. Lowe, A.M. Al-Jumaily, *J. Material. Sci. Eng.* **5**, 254 (2016).
[22]. K. Khaothong, In: C.T. Lim, J.C.H. Goh (eds) *6th World Congress of Biomechanics (WCB 2010), IFMBE Proceedings* **31**, (Springer, Berlin) pp. 1467-1470.
[23]. Y. Zheng, A.F.T. Mak, *IEEE Eng. Med. Biol. Soc.* **7**, 257 (1999).
[24]. P. Sangsanoh, O. Suwantong, A. Neamnark, P. Cheepsunthorn, P. Pavasant, P. Supaphol, *Eur. Polym. J.* **46**, 428 (2010).
[25]. T. Zhou, N. Wang, Y. Xue, T. Ding, X. Liu, X. Moc, J. Suna, *Colloids Surf. B Biointerfaces* **143**, 415 (2016).
[26]. M. Kempf, Y. Miyamura, P.Y. Liu, A.C.H. Chen, H. Nakamura, H. Shimizu, Y. Tabata, R.M. Kimble, J.R. McMillan, *Biomaterials* **32**, 4782 (2011).
[27]. K.S. Rho, L. Jeong, G. Lee, B.M. Seo, Y.J. Park, S.D.Hong, S. Roh, J.J. Cho, W.H. Park, B.M. Min, *Biomaterials* **27**, 1452 (2006).
[28]. J. Pelipenko, P. Kocbek, J. Kristl, *Eur. J. Pharm. Sci.* **66**, 29 (2015).
[29]. J. Pelipenko, P. Kocbek, B. Govedarica, R. Rošic, S.Baumgartner, J. Kristl, *Eur. J. Pharm. Biopharm.* **84**, 401 (2013).
[30]. P. Bhattacharjee, D. Naskar, H.W. Kim, T.K. Maiti, D. Bhattacharya, S.C. Kundu, *Eur. Polym. J.* **71**, 490 (2015).
[31]. N.M. Alves, I. Pashkuleva, R.L. Reis, J.F. Mano, *Small* **6**, 2208 (2010).